Weierstraß-Institut

für Angewandte Analysis und Stochastik

im Forschungsverbund Berlin e. V.

Rotational symmetry breaking in small-area circular vertical cavity surface emitting lasers

Ihar Babushkin, Uwe Bandelow, Andrei G. Vladimirov

submitted: 14.07.2010

Weierstrass Institute
for Applied Analysis and Stochastics
Mohrenstr. 39
10117 Berlin
Germany
E-Mail: ihar.babushkin@wias-berlin.de

Abstract

We investigate theoretically the dynamics of three low-order transverse modes in a small-area vertical cavity surface emitting laser. We demonstrate the breaking of axial symmetry of the transverse field distribution in such a device. In particular, we show that if the linewidth enhancement factor is sufficiently large dynamical regimes with broken axial symmetry can exist up to very high diffusion coefficients ~ 10 μm^2/ns.

1   Introduction

In the last decades, vertical cavity surface emitting lasers (VCSELs) have attracted continuous attention due to their promising applications as high power ultra-compact coherent light sources. Unlike edge emitting lasers VCSELs can be made rather homogeneous in the transverse direction, which can lead to a complicated dynamics of transverse modes. In the present article we consider an axially symmetric VCSEL with relatively small aperture radius (~ 2 μm). Typically, it is expected that the fundamental transverse mode dominates in the output of such a device, at least close enough to the lasing threshold. That is, the intensity profile is axially symmetric. The appearance of higher-order transverse modes can break the axial symmetry, at least in the instantaneous field (the symmetry can be restored by time averaging of the dynamics in certain cases). In this article we show that even in such small-aperture devices the higher-order modes can be excited despite of the strong influence of carrier diffusion and boundary conditions, leading to asymmetric emission from an axially symmetric device.

Interaction between few laser modes in the presence of a spatial population grating were reported earlier for different class B laser models. In particular, in [1, 2] a transition to antiphase pulsations of two counterpropagating waves resulting from frequency detuning was demonstrated in a bidirectional class B laser. Bifurcation mechanisms underlying this transition were described in [3]. In [4] a solid-state class B laser with circular aperture was considered. It was shown that even under symmetric pump conditions the break-up of axial symmetry can take place when the pump is "broad enough", i.e. when the overlap integral of the pumping field with the higher-order cavity modes is sufficiently large. A similar phenomenon was predicted for the off-axis LP (linearly polarized) waves in a broad-area VCSEL in [5]. In addition, many details of the carrier dynamics including diffusion were taken into account in more comprehensive VCSEL modeling approaches [6, 7, 8, 9, 10, 11]. However, the complexity

1

of these models prevented the authors from systematical study of large parameter ranges.

In the present article we study the effect of the carrier diffusion and linewidth enhancement factor [12] on the dynamics of three lowest-order transverse modes of small-aperture VCSELs in a wide parameter range. We show that for sufficiently high diffusion coefficients the fundamental mode always dominates in the laser dynamics. The appearance of higher-order modes is, however, possible even for rather high diffusion coefficients $\sim 10\ \mu\mathrm{m}^2$/ns, provided that the linewidth enhancement factor is large enough. In general, the α-factor plays a destabilizing role in the laser dynamics leading to a destabilization of cw states, see, e.g. [2, 5]. In particular, with the increase of this factor the range of diffusion coefficients where nontrivial dynamical regimes exist increases.

2 The basic equations

Assuming linear polarization of laser radiation, we start from the scalar variant [5] of the vectorial equations [13, 14] governing the spatio-temporal evolution of the field $e(\mathbf{r}_\perp, t)$ and of the carrier density $d(\mathbf{r}_\perp, t)$ in a VCSEL:

$$\dot{e} = -\kappa e - i\hat{\Omega}e + \kappa(1+i\alpha)d\mathscr{L}e, \tag{1}$$

$$\dot{d} = -d + j - de^*\hat{\mathscr{L}}(de) + D_f\Delta_\perp d. \tag{2}$$

Here the time t is normalized to the carrier relaxation time, $\mathbf{r}_\perp = \{r, \phi\}$ are radial coordinates in transverse plane, κ is the cavity decay rate, α is the linewidth enhancement factor and $\Delta_\perp = \frac{1}{r}\frac{\partial}{\partial r}\left(r\frac{\partial}{\partial r}\right) + \frac{1}{r^2}\frac{\partial^2}{\partial \phi^2}$ is the transverse Laplacian. The operators $\hat{\Omega}$ and $\hat{\mathscr{L}}$ are defined for every transverse mode $e = \psi_{mn}$ as $\hat{\Omega}\psi_{mn} = \delta_{mn}\psi_{mn}$ and $\hat{\mathscr{L}}\psi_{mn} = \psi_{mn}/(1 + \delta_{mn}^2/\gamma^2)$, where δ_{mn} is the detuning of the mode ψ_{mn} and γ is the normalized polarization decay rate. The parameter $j(\mathbf{r}_\perp, t)$ stands for the injection current density and D_f is the diffusion coefficient normalized to the mode diameter (see below for the discussion of the mode shapes). We will limit our analysis to the dynamics of three lowest-order transverse modes: the fundamental mode and two first order ones. The onset of the first order modes causes the axial symmetry breaking in the system under study. In Eqs. (1)-(2), the threshold value for the fundamental mode is $j = 1$. Following Ref. [4], we substitute $d = 1 + n$, where n is the excess of carrier density above the threshold value, into Eqs. (1)-(2), neglect higher-order nonlinear terms

[3], and write the equations for the relevant modal amplitudes:

$$\dot{F}_0 = -\kappa F_0 + 2\kappa(1+i\alpha)L_0 F_0 M_0, \tag{3}$$

$$\dot{F}_+ = -\kappa F_+ + \kappa(1+i\alpha)(L_+ F_+ N_0 + L_- F_- N_2), \tag{4}$$

$$\dot{F}_- = -\kappa F_- + \kappa(1+i\alpha)(L_- F_- N_0 + L_+ F_+ N_2^*), \tag{5}$$

$$\dot{M}_0 = -M_0 + j_{m_0} - 2D_{f01}M_0 + D_{f01}N_0 -$$
$$- (2\Theta_0 L_0 |F_0|^2 + \Theta_1 L_- |F_-|^2 + \Theta_1 L_+ |F_+|^2), \tag{6}$$

$$\dot{N}_0 = -N_0 + j_{n_0} - 2D_{f11}N_0 + \frac{1}{4}D_{f11}M_0 -$$
$$- (\Theta_1 L_0 |F_0|^2 + \Theta_2 L_- |F_-|^2 + \Theta_2 L_+ |F_+|^2), \tag{7}$$

$$\dot{N}_2 = -N_2 + j_{n_2} - \Theta_2 L_+ F_+ F_-^* - 2D_{f11}N_2 - \frac{1}{4}D_{f11}M_0. \tag{8}$$

Here $F_0 \equiv \psi_{00}\exp(i\delta_{00}t)$ is the (complex) amplitude of the fundamental axially symmetric transverse mode and $F_{\pm} = \psi_{0\pm1}\exp(i\delta_{0\pm}t)$ are the amplitudes of two first order modes.

In Eqs (3)-(8) the variables $M_0 = N_{0000}$, $N_0 = N_{0101}$, and $N_2 = N_{010-1}$, describe different harmonics of the spatial population grating in the transverse plane. $\Theta_0 = \Theta_{0000}^{0000}$, $\Theta_1 = \Theta_{0101}^{0000}$, $\Theta_2 = \Theta_{0101}^{0-10-1}$, $D_{fij} = D_f \mu_{ij}^2$ with μ_{ij} defined by the boundary conditions. These quantities are given by

$$N_{nmn_1m_1} = \int_S \psi_{mn}^* n \psi_{m_1n_1} r\,dr\,d\phi, \tag{9}$$

$$\Theta_{mnm_1n_1}^{m_2n_2m_3n_3} = \int_S \psi_{mn}^* \psi_{m_1n_1} \psi_{m_2n_2}^* \psi_{m_3n_3} r\,dr\,d\phi, \tag{10}$$

$$j_{m_0} = \int_S j|\psi_{00}|^2 r\,dr\,d\phi, \quad j_{n_0} = \int_S j|\psi_{01}|^2 r\,dr\,d\phi, \tag{11}$$

$$j_{n_2} = \int_S j\psi_{01}^* \psi_{0-1} r\,dr\,d\phi, \tag{12}$$

where integration is performed over the cross-section area of the VCSEL.

In our numerical simulations we have used the following parameter values of the VCSEL under consideration. The oxidation aperture with the radius $R \approx 2.5\ \mu$m is placed on the top mirror. The outer part of the cavity is defined by etching at $R_{et} \approx 13\ \mu$m. Determination of the mode shape in such a VCSEL structure is a rather complex problem [6, 7, 12, 17, 18, 19]. The mode shape is influenced by the index step aperture, etching aperture, injection current profile, and dynamical effects such as thermal lensing. Therefore, for the sake of generality we consider here two different sets of modes: the Bessel modes defined by the oxidation layer and the Laguerre-Gaussian modes with the same waist. In both cases the diffusion coefficient D_f is normalized to the aperture width R. For the Bessel modes we have $\Theta_0 \approx 0.668$, $\Theta_1 \approx 0.456$, $\Theta_2 \approx 0.494\ldots$, and μ_{ij} is the ith root of the Bessel function of jth order. For the Laguerre-Gaussian modes the coefficients of Eqs. (3)-(8) are very similar: $\Theta_0 = \Theta_1 = \Theta_2 = 1/2$. We will show that the results are qualitatively independent of the choice of the mode shape.

3

For the presentation clarity, we assume also zero detuning between the two first order transverse modes in Eqs. (3)-(8) which is the case when the pumping and device structure is axially symmetric. In addition, we assume that the spectral width of the gain contour is larger than the detuning between the fundamental and the first-order transverse modes and that the highest-order pump parameter j_{n_2} is neglectable.
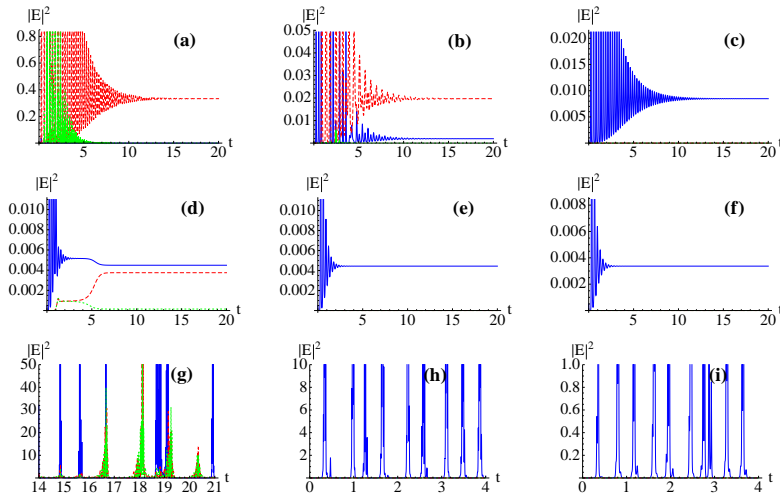
3   Simulations

Figure 1: (Color online) Modal intensity timetraces obtained numerically using Eqs. (3)-(8). $R = 2.5$ μm. Different panels correspond to different values of the parameters ε, D, and α. (a)-(c) $D = 0$, $\alpha = 0$. (d)-(f) $D_f = 40$ ns/μm^2, $\alpha = 0$. (g)-(i) $D = 4.0$ μm^2/ns, $\alpha = 3$. (a),(d),(g) $\varepsilon = 0.4$. (b),(e),(h) $\varepsilon = 1.2$. (c),(f),(i) $\varepsilon = 3$. The fundamental mode is shown by the solid blue line, whereas the two first order modes are shown by red dashed and green dot-dashed lines, respectively. The pump parameter is $j_{m0} = 5.9$ (except (g), where $j_{m0} = 1.7$). In (g) the intensities for F_+ and F_- are amplified 100 times to increase the visibility.

As it was demonstrated in [4], the dynamics of the transverse modes in a class B laser strongly depends on the ratio $\varepsilon = j_{m0}/j_{n0}$, i. e. on the relative "width" of the pumped area. Our simulations show that if $D_f \neq 0$ the fundamental mode always dominates near the lasing threshold. Therefore, we consider here quite strong pumping 2-3 times larger than the threshold one. In Fig. 1(a)-(c) three typical timetraces of modal intensities calculated numerically for $D_f = 0$ and $\alpha = 0$ are shown. The so-called "running wave" solution corresponding to zero amplitude of the fundamental mode, $|F_0|^2 = 0$, and nonzero amplitude of one of the first order modes, $|F_-|^2$ or $|F_+|^2$, see Fig. 1(a), is stable for $\varepsilon \lesssim 0.9$. For $\varepsilon \gtrsim 2.0$ the fundamental mode solution ($|F_0|^2 > 0$, $|F_-|^2 = 0$, $|F_+|^2 = 0$) becomes stable, see Fig. 1(c). In the intermediate range of ε a stable mixed solution with nonzero amplitudes of all three transverse modes [$|F_0|^2 > 0$ and $|F_-|^2 > 0$ or $|F_+|^2 > 0$, see Fig. 1(b)] exists.

4

The timetraces shown in Fig. 1(d)-(f) correspond to a nonzero diffusion coefficient $D_f = 40\ \mu\text{m}^2/\text{ns}$. As one can see, typically the contribution of the fundamental mode into the laser field increases with the diffusion coefficient. In particular, the running wave regime is transformed into the mixed wave one [cf. Fig. 1(d) and Fig. 1(a)], and a mixed wave regime – into the fundamental mode regime [cf. Fig. 1(e) and Fig. 1(b)]. Furthermore, due to additional damping introduced by the carrier diffusion in Eqs. (3)-(8) the amplitude of the solution becomes smaller and starting from the same initial condition the system approaches the cw solution much faster than in the absence of the diffusion. This means in particular, that the carrier diffusion suppresses dynamic instabilities. Similar behavior was reported earlier for a bidirectional class B ring laser [1].
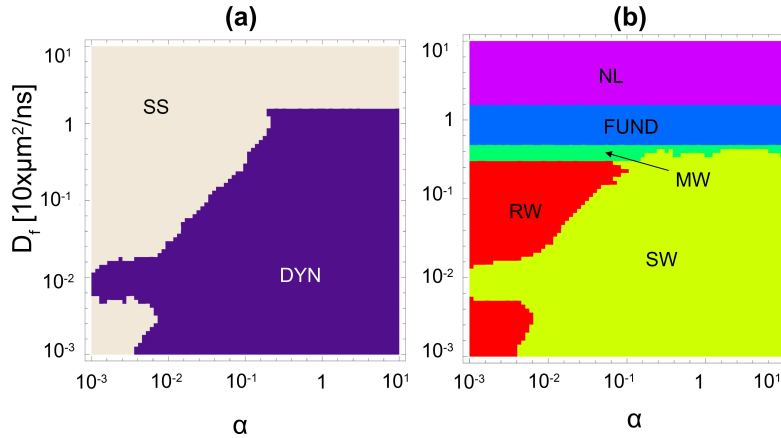

Figure 2: (Color online) Numerically calculated regions of different laser operation regimes on $\{\alpha, D_f\}$-plane for $j_{m0} = 5.9$ and $\varepsilon = 0.4$. (a) CW vs. dynamical (DYN) regimes. (b) Regions corresponding to different amplitudes of transverse modes. NL: $|F_0|^2 = 0$, $|F_+|^2 = 0$, $|F_-|^2 = 0$ (non-lasing solution); FUND: $|F_0|^2 \neq 0$, $|F_+|^2 = 0$, $|F_-|^2 = 0$ (fundamental mode); MW: $|F_0|^2 \neq 0$, $|F_+|^2 \neq 0$, $|F_-|^2 \neq 0$ (mixed wave); SW: $|F_0|^2 = 0$, $|F_+|^2 \neq 0$, $|F_-|^2 \neq 0$ (standing wave); RW: $|F_0|^2 = 0$ and one of $|F_+|^2$ or $|F_-|^2$ is nonzero (running wave).

In the presence of nonzero α-factor the dynamics of Eqs. (3)-(8) changes significantly. In particular, it is well know that the cw solution becomes unstable for sufficiently large $\alpha \neq 0$ [2, 5]. This is illustrated by Fig. 1(g)-(i) which corresponds to $\alpha = 3$. One can see that well developed dynamical pulsations consisting of short peaks of either only the fundamental mode intensity, see Fig. 1(h)-(i), or the intensities of all three transverse modes, see Fig. 1(g).

The diagrams in Fig. 2 present the regions of different dynamical regimes of Eqs. (3)-(8) in the plane of two parameters, namely the diffusion coefficient D_f and the linewidth enhancement factor α. In Fig. 2(a) the cw solutions (CW) and dynamical regimes with time dependent modal intensities (DYN) are shown by different colors. One can see that for $D_f \lesssim 2\ \mu\text{m}^2/\text{ns}$ a transition to dynamical regimes takes place for sufficiently large values of the linewidth enhancement factor α. Regimes with different

modal amplitudes are indicated by different colors in Fig. 2(b). As it is seen from this figure, for $2 \lesssim D_f \lesssim 20\ \mu\mathrm{m}^2/\mathrm{ns}$ a cw solution corresponding to the pure fundamental mode is stable (see the blue region indicated FUND). At even stronger diffusion the laser stops to lase for the chosen pump rate (see the violet region NL). In a small region below $D_f \approx 2\ \mu\mathrm{m}^2/\mathrm{ns}$ the stable solution consists of all the three transverse modes. At even smaller diffusion coefficients D_f, a "running wave" (RW) regime, which is typically a cw solution [cf. Fig. 2(a)] corresponding to a single first order transverse mode, is stable for sufficiently small values of the linewidth enhancement factor α. For larger α a regime with zero fundamental mode amplitude and antiphasely oscillating amplitudes of the two first order modes establishes. This regime is denoted as MW ("mixed wave") in Fig. 2(b). The existence of similar oscillations was predicted theoretically for a class B laser operating at three [4] and two [20] transverse modes, as well as for other laser geometries [1, 2, 5].

In the simulations described above Bessel modes have been used. We have recalculated the diagrams shown in Fig. 2 for the case of Laguerre-Gaussian modes, see discussion after Eq. (9). The resulting diagrams are very similar to those shown in Fig. 2, with the only difference that all the colored regions are shifted as a whole to the direction of larger diffusion. Therefore, we assume, that the behavior described above is rather generic.

4 Conclusions

To conclude, we considered the dynamical regimes arising in a small-area index-guided VCSEL. We showed that the symmetry breaking bifurcation predicted in [4] is still possible in this device for the values of the diffusion coefficient up to $\sim 10\ \mu\mathrm{m}^2/\mathrm{ns}$. The presence of the linewidth enhancement factor in the model equations leads to the appearance of dynamical regimes, that can involve fundamental as well as first order transverse modes. Carrier diffusion has a tendency to increase the lasing threshold and to stabilize CW regimes. The dynamics remains qualitatively insensitive to the exact mode shape (Bessel vs Laguerre-Gaussian modes). This stabilizing behavior is somewhat similar to that of the cavity solitons and their bound states in semiconductor lasers predicted in [21, 22, 23].

References

[1] I. V. Korukin *et al.*, Quant. Elektron., **22**, 11 (1995).

[2] Ya. I. Khanin, *Fundamentals of Laser Dynamics*, Cambridge Int Science Publishing, 2005.

[3] A. G. Vladimirov, Opt. Commun. **149**, 67 (1998).

[4] A. G. Vladimirov and D. V. Skryabin, Quant. Electron. **24**, 913 (1997).

[5] I. Babushkin and N. A. Loiko, PRA 67, 013813 (2003).

[6] A. Valle, IEEE J. Quant. Electron., **34** 1924 (1998).

[7] J. Mulet and S. Balle, Phys. Rev. A., **66**, 053802 (2002).

[8] J. Mulet and S. Balle, IEEE J. Quant. Electron., **38**, 053802 (2002).

[9] O. Hess and T. Kuhn, Phys. Rev. A, **54**, 3347 (1996).

[10] C. Z. Ning and P. M. Goorjian, J. Opt. Soc. Am. B, **16** 2072(1999).

[11] T. Rössler *et al.*, Phys. Rev. A, **58**, 3279 (1998).

[12] C. H. Henry, J. Quant. Electron., **18** 259 (1982).

[13] M. San Miguel, Q. Fend and J. V. Moloney, Phys Rev A. **25**, 1728 (1995).

[14] N. A. Loiko and I. V. Babushkin, J. Opt. B: Quant. Semiclass. Opt. 2001.

[15] J. Moloney, J. Opt. B: Quant. Semiclass. Opt., **1**, 183(1999).

[16] A. W. Snyder and J. D. Love, *Optical waveguide theory*, Springer, 1983.

[17] D. I. Babic and S. W. Corzine, IEEE J. Quant. Electron., **28**, 514 (1992).

[18] D. I. Babic *et al.*, IEEE J. Quant. Electron., **29**, 1950 (1993).

[19] R. Riyopoulis *et al.*, JOSA B 18, 1268 (2001).

[20] D. Skryabin and A. G. Vladimirov, Quant. Electron. 24, 918 (1997).

[21] A. G. Vladimirov, G. V. Khodova, and N. N. Rosanov, Phys. Rev. E, **63**, 056607 (2001).

[22] D. V. Skryabin, and A. G. Vladimirov, Phys. Rev. Lett. **89**, 044101, (2002).

[23] I. Pérez-Arjona et al, Opt. Express, **17**, 4897(2009).